

## Article

# The Resistance of Welded Joints of Galvanized RHS Trusses with Different Vent Hole Geometries

Miguel A. Serrano <sup>1,\*</sup> , Carlos López-Colina <sup>1</sup> , Fernando L. Gayarre <sup>1</sup>, Tim Wilkinson <sup>2</sup> and Jesús Suárez <sup>1</sup>

<sup>1</sup> Department of Construction and Manufacturing Engineering, University of Oviedo, Campus de Gijón, 33203 Gijón, Spain; lopezpcarlos@uniovi.es (C.L.-C.); gayarre@uniovi.es (F.L.G.); suarezg@uniovi.es (J.S.)

<sup>2</sup> School of Civil Engineering, University of Sydney, Sydney NSW 2008, Australia; tim.wilkinson@sydney.edu.au

\* Correspondence: serrano@uniovi.es; Tel.: +34-985181947

Received: 18 March 2019; Accepted: 9 April 2019; Published: 15 April 2019



**Featured Application:** This work will help designers to decide the best geometry and position for the vent holes in galvanized tubular trusses. Galvanizing associations at a national and international level will clearly benefit from the results derived from this research.

**Abstract:** A worldwide-accepted technique to protect steel lattice girders with welded hollow sections against corrosion is the hot-dip galvanizing process. In this process, vent holes are required in braces to fill the inner part protecting them from corrosion, to allow the immersion of the structure in the zinc bath and to recover the excess fluid after the bath. The cross-section reduction due to the vent hole could lead to a decrease in the effective brace resistance; this is not easily quantified, because there are neither prescriptions nor recommendations in the design codes to assess this effect. Therefore, the hollow structural sections could be underutilized due to doubts regarding the safety of this type of joint. This research was conducted in order to categorize different geometries and positions of vent holes in order to determine the best in terms of joint efficiency. A validated finite element model considering welds on lattice girders joints was extended to take into account different vent hole shapes. This research concludes that the presence of ventilation holes such as the ones considered in this study does not significantly affect the joint resistance, and that all the analyzed hole shapes could be proposed as a valid solution for machining vent holes. The conclusions drawn up from this work could be useful for structural steel designers, providing them with valuable design recommendations.

**Keywords:** galvanized structures; welded joints; hollow sections; numerical simulation; vent holes

## 1. Introduction

There are several techniques for protecting steel structures against corrosion. However, when the structure to be protected is a steel lattice girder in which the chords and braces are hollow sections, the most cost-effective protection technique is probably the hot-dip galvanizing process. Although the term ‘galvanizing’ has been widely used to describe the coating of steel with zinc, it is necessary to clear up some misconceptions, as discussed in [1]. The process of hot-dip galvanizing (HDG) requires the immersion of the structure, which has been cleaned previously, in a big kettle containing a bath of molten zinc at a temperature of 450 °C [2]. The structure is introduced into the kettle at an angle, which allows the air to move inside the hollow sections and to escape at the same time as the zinc is flowing into those sections. A reaction between the iron in the steel and the zinc produces some intermetallic layers, which create a barrier with the environment and cathodically protect the steel. A coating is formed that provides protection for both the inside and outside of the pieces, not only

for the flat surfaces, but also for the corners and edges of the tube, ensuring a long maintenance-free service life that can be extended for 75 years in most environments [3]. As a result, the Life-Cycle Cost (LCC) of these structures remains the same as its initial cost. This is an advantage of the HDG when compared with other systems of protection when considering the Life-Cycle Cost.

In the case of a lattice girder, an alternative could be to separately galvanize the brace members and to weld them onto the chords later. Nevertheless, the welding process for galvanized pieces requires them first to be brushed in order to remove the coat, then to be welded, and finally to be sprayed with a coat or a paint with a high zinc content. This results in a lower-quality coating when compared with the results obtained by immersion of the whole structure in a kettle. Furthermore, the increasing capabilities of galvanizing plants make the immersion of a full structure or a part thereof the best options in the specific case of lattice girders.

Then, if a lattice girder with hollow chords and braces needs to be galvanized, their braces have to have been machined previously in order to produce ventilation holes in the proximity of the welded connection, or even interrupting the welds. Vent holes are required to fill the inner part of the brace members to protect them from corrosion. They are also necessary to allow the immersion of the structure in the zinc bath and to recover excess fluid after the bath so that it can be reused. In this situation, the holes should be big enough to efficiently fulfil the requirements described, but it is important to be aware of the potential reduction in joint strength in the case of excessive hole size.

There are no prescriptions or practical recommendations in the design codes [4–6], standards [7,8], or design guides for hollow structural sections [9–12]. So inevitably, there are some doubts among structural steel designers with respect to the effect of vent holes on joint resistance, and this lack of knowledge may reduce the use of galvanized lattice girders, despite their high efficiency.

The range of applications for hollow steel sections (HSS) in general, and rectangular hollow sections (RHS) more specifically, has increased noticeably in recent decades, and covers many types of construction—particularly trusses—due to certain advantages [13], not only with respect to member design, but also associated with joint design [14]. With regard to the selection of hot-finished or cold-formed manufacturing methods for hollow sections, Puthli and Packer [15] concluded that as long as the products are in accordance with European standards [7,8] and the design is carried out sensibly, cold-formed products perform efficiently in all structural applications. More specifically, in truss joint design, where the joint resistance typically governs the selection of hollow section members, any superior compressive resistance achievable by hot-finished products is frequently not utilized. Furthermore, protection against corrosion and welding around the corners of brace members when they are welded to the chord of the lattice girder is easier to achieve in cold-formed sections due to their smoother corner radius. In the same way, according to [16], the manufacturing method, hot-finished or cold-formed, is not the fundamental factor dictating the properties of hollow sections. Ritakallio [16] studied the suitability of cold-formed tubes for structural applications, and specifically considered the suitability of these products to be hot-dip galvanized due to their potential risk of corner cracking, which is sometimes associated with this protection process. The conclusion of this publication was that properly made cold-formed hollow sections do not have a tendency to LME (liquid metal embrittlement), and corner cracking and hot-dip galvanizing do not essentially alter the strength or the ductility of the hollow sections. Therefore, welded structures made of cold-formed hollow sections can be safely protected using the hot-dip galvanizing process.

According to the European General Galvanizers Association (EGGA) [17,18], the use of galvanization in Europe is strong, and exhibited an increase of about 25% within a period of 15 years, reaching a maximum of nearly 7.0 million tons in 2008. After that peak in production, and as a consequence of the economic crisis in Europe, there was a reduction of around 7%, since when the prospects in major European countries have not been so encouraging. Nevertheless, it is hoped that further market penetration against painting of steel will continue.

Researchers studying the effect of hot-dip galvanizing on steel properties have concluded that the effect of the process on the main mechanical properties, such as yield limit, is almost negligible [19].

As a result, the standard specifications (ASTM A924 and EN10142) calculate the yield and tensile strengths for hot-dip coated steel using the base steel thickness only [20]. Although pre-galvanizing countermeasures should be considered to avoid cases of brittle cracking resulting from hot-dip galvanizing on cold-formed tubes [21,22], when the process is carried out correctly, this embrittlement effect has been found to be negligible, even in hot-dip galvanized welded joints submitted to fatigue loads [23]. Together with all the previous statements, we can assume that the heat-affected zone (HAZ) in structural steel, and particularly in HSS, does not affect the welded joint behavior [24].

According to the previous paragraphs, the main gap of knowledge with respect to hot-dip galvanized trusses with hollow sections is the effect of the vent holes on the resistance of the welded joints, since most of the other effects of the zinc bath are negligible when the process is performed correctly. Some research has been carried out in the framework of two projects [25,26] funded by the CIDECT (Comité International pour le Développement et l'Etude de la Construction Tubulaire) and the EGGA (European General Galvanizing Association). In [25], after a deep literature review, the authors suggested the most appropriate sizes, shapes and positions of ventilation holes, although they did not study joint resistance. In [26,27], a study based on an extensive experimental program and subsequent finite element analysis studied whether or not the circular holes recommended in [25] produced a reduction in the joint resistance of different configurations of typical welded truss joints involving RHS with gaps between the braces. The main result suggested that the considered vent holes had a very small effect on the joint strength. In that research, circular holes located away from the chord face were considered. This type of vent hole does not decrease the perimeter welds of the braces, which allows good structural response, but makes it impossible to recover any of the fluid zinc. With the aim of improving this drawback and looking for the best shape of the holes, a new step forward was carried out in [28]. However, considering the conclusions of the many pieces of research on hollow sections that can be found in the bibliography, that initial model required further improvement before being able to provide enough consistency in any conclusions that could have arisen from it. The improvements that are proposed in the present new research work are as follows:

- The numerical model needed to be validated against experimental results. For this purpose, the main source of experimental values for the development of design equations for welded joints of RHS trusses (i.e., the Delft University test reports) was used. Six tests on K gap joints between RHS were selected, because their observed failure was related to the so-called “brace failure” of K welded joints between RHS, which involves both the effective width failure and the local buckling failure on the brace elements. This is because they are clearly the failure modes that are expected to be more influenced by the presence of holes in the brace.
- As is clearly stated in the bibliography, in most cases, weld geometry must be modeled in situations where the gaps between the braces are important. However, this was not really modeled in the previous work mentioned, which only considered an estimation of the thermal effects of the weld process. This lack of geometrical weld modeling is solved in this new paper, and the thermal effects mentioned were neglected, since neither the bibliography nor the previous work carried out by the authors [24] showed any appreciable influence of this factor.
- The general design of the experiment presented in the previous work was not specifically focused on failure modes that could be more greatly affected by the vent holes. Nevertheless, in the present paper, a parametric study has been designed by selecting joints that, according to the design equations, could represent “brace failure” or, in some cases, the “chord face failure”, which is very close to a “brace failure”.
- The brace lengths in the models of the previous work led to brace buckling in some cases, but not local buckling at the connection location. The brace lengths were reduced in the present work to ensure that the results really showed joint failures.
- Elliptical holes were not considered in this work, because they are impractical.
- Finally, in this new paper, not only K-joints, but also N-joints were considered.

Now, in this new paper, a detailed analysis has been carried out to categorize some different geometries and to determine the best of them in terms of joint efficiency for the K- and N-welded joints, which are present in Warren and Pratt trusses, respectively, which are the two most widely used lattice girders. For this purpose, a finite element model was validated using the results of experimental testing on welded joints between RHS, and then it was extended to take into account the proposed vent hole geometries.

The K-joints and N-joints are considered under static loading only. Fatigue loads are not within the scope of this paper. It is worth mentioning that, according to the design codes for trusses in many building structures and some industrial applications, they may be designed considering just static loading. These type of structures with galvanizing vent holes are the focus of this research and some practical recommendations can be extracted from this work.

## 2. Finite Element Modeling

The general-purpose finite element software Ansys Workbench (Ansys Inc, Canonsburg, Pennsylvania, PA, USA) was used to carry out a numerical analysis to determine the most efficient geometry of vent holes with respect to both the joint resistance and the amount of molten zinc recovered. The model complexity in cases of welded joints between RHS can vary, and ranges from shell elements at the mid-surface of the faces without any element simulating the weld bead through to solid 3D elements including the welds [29]. In the case of T and X joints, the simplest option (shell elements without welds) has been demonstrated to be sufficiently accurate to obtain the static strength of joints [30]. However, the most common truss joints (K- and N-type) have two braces welded to a chord, and the consideration of the actual gap between welds—not only between the chord faces—is essential to evaluating their strength, especially when these gaps are appreciable. Multiple simplified shell models were tested [29–34], and the best approximations without increasing complexity were those based on the proposals made by Van der Vegte et al. [32] or by Lee and Wilmshurst [33]. The inclusion of the welds in numerical models of steel tubular trusses is also important when considering cyclic loads, as it is necessary in cases where there is some damage to the constitutive model of the welded joints [34].

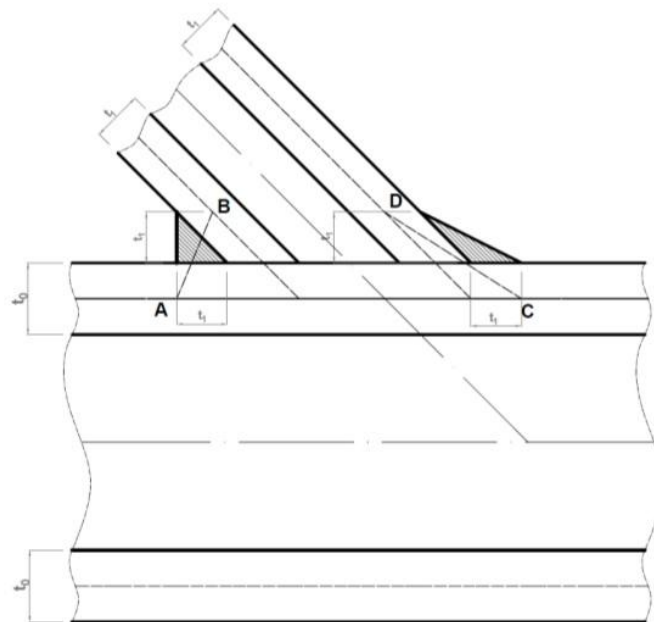
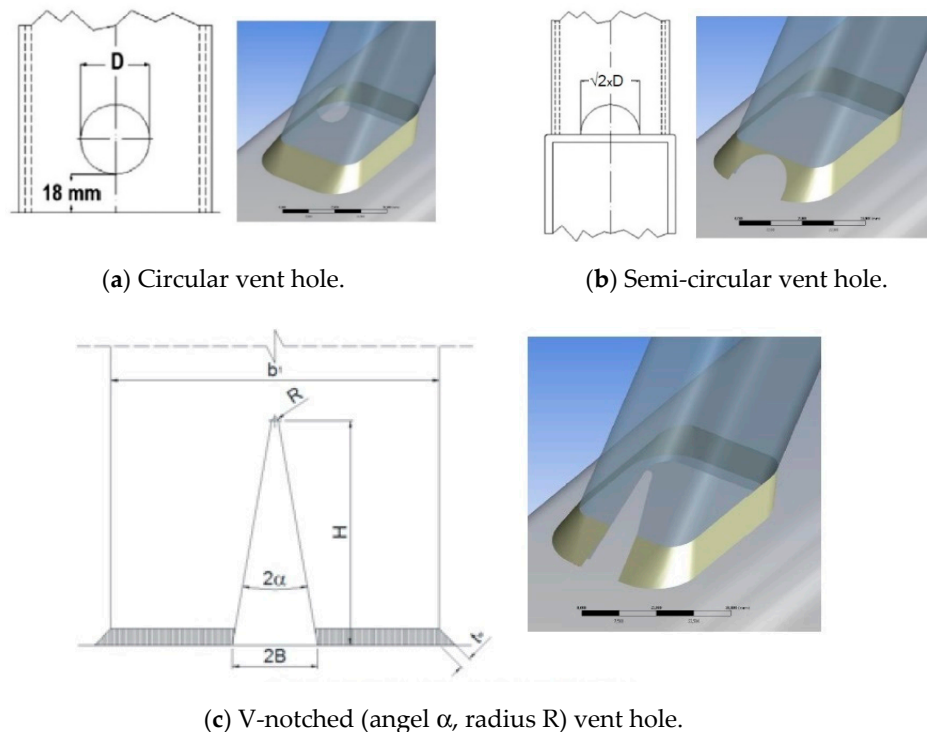


Figure 1. Weld geometry modeling with shell elements (A–B and C–D).

To obtain an accurate and efficient simulation, the effect of welds in reducing the gap, and thereby stiffening the joint, was ultimately modeled in this research work by means of a ring of shell elements around the braces based on the geometry proposed by the latter authors [33], as presented in Figure 1.

The thickness adopted for the shell elements of the welds was equal to the chord thickness. In practical terms, this is similar to the weld throat proposed by the CIDECT for joints between hollow sections [9].

K-joints and N-joints were considered in this work. For either of these, four different models, selected depending on vent hole presence or geometry, were analyzed. All of the studied joints included a parametrically variable gap that was dependent on the rest of the joint dimensions. The first model did not include any vent holes and was used to validate the numerical model on the basis of a comparison with test results. Once the initial model was validated, it was extended to consider three different vent hole geometries and positions in order to determine the best proposal. Figure 2 shows these three configurations. Figure 2a shows a circular hole of diameter  $D$ , located 18 mm away from the chord face, which was the same location considered in our previous work [26,27]. This configuration reduces the stress concentration around the hole and does not shorten the weld length; on the other hand, some liquid is retained inside the brace. Figure 2b shows a semicircular hole with a diameter of  $\sqrt{2} \times D$  to maintain the same filling area as the previous circular one. Figure 2c shows a V-notched vent hole that presents a lower cut-off of the weld when compared with the semicircular hole, while maintaining the same filling area as the other two proposals. The two configurations shown in Figure 2b,c allow the total recovery of liquid after the galvanization process, but they need to cut off the weld between the braces and the chord. As stated previously, the three geometries maintain the same filling area. This area always refers to the area of the circular hole, whereby the diameter  $D$  was assumed to be 25% of the X-section diagonal of the corresponding brace, in accordance with the recommendations in [25]. Therefore, in the case of a semicircular hole, the diameter is  $\sqrt{2} \times D$ . Nevertheless, for the V-notched configuration, some new design variables were taken into account (Figure 2c). These are the dimensions  $2B$ —that is, the maximum opening—and  $H$ , which is the height of the notch. Both dimensions depend on the angle  $\alpha$ , the radius  $R$ , and the diameter  $D$  to maintain the filling area.



**Figure 2.** Configuration of different vent holes.

Equations (1) and (2) allow the calculation of  $B$  and  $H$ . In the models for the numerical simulation, a radius of 1 mm and an angle  $\alpha$  of  $10^\circ$  were considered.

$$B = \sqrt{\left(\frac{\pi D^2}{4} + \frac{R^2}{\tan \alpha} - \pi R^2 \left(\frac{180 - 2\alpha}{360}\right)\right) \tan \alpha} \quad (1)$$

$$H = \frac{B}{\tan \alpha} - \frac{R}{\sin \alpha} \quad (2)$$

To create the meshes of the models, 181 shell elements, with four nodes and six degrees of freedom per node, were chosen. These shell elements have already proved their suitability in the simulation of thin-walled hollow sections in [27] and [35–37]. In [38], the authors' conclusions agreed with those of many previous researchers [39], and concluded that shell elements provide satisfactory results for the simulation of welds in RHS, and offer an important saving in computation time compared with solid elements. It is important that the element size fits the requirements of the simulation, so a finer mesh of 3 mm was taken in the proximity of the joint; more specifically, within a sphere with a diameter of 150 mm centered on the point of axis concurrence. Two additional refinements of the meshes were also carried out for welds and around the hole borders. The detailed calibration carried out on models involving RHS and fillet welds [38] supports the selection of this mesh size, making it possible to develop models with fewer than 30,000 elements and nodes in all cases. Parametric models were developed, enabling their adaptation to specific joints. Figure 3 shows the four meshed models with the three-vent-hole configurations.

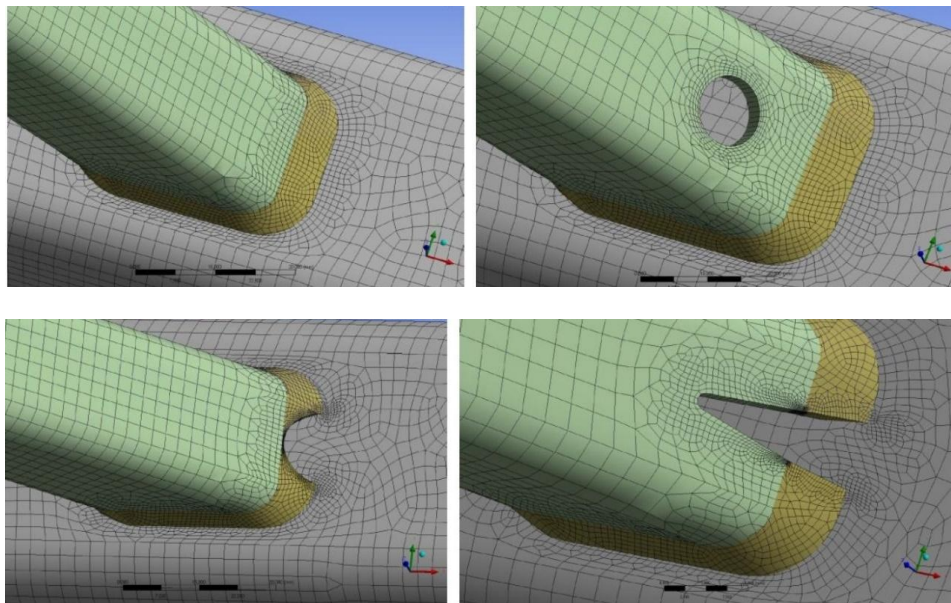


**Figure 3.** Mesh models of holes and welds.

Figure 4 shows the global boundary conditions adopted in the case of a symmetric K-joint. A progressive load was applied directly on the brace member until the maximum load and subsequent failure were reached. To simulate this, small steps of displacement were introduced on the end of the brace under compression. A displacement was applied axially along the brace, while the other two local axis displacements for this member were restrained. The end of the brace member under tension and the end of the chord under compression (the right part of the chord in Figure 4) were pinned in the center of their faces. The other end of the chord (the left part in Figure 4) was free in plane, while the out-of-plane axis displacement was restrained. The boundary conditions adopted made it possible to reproduce the test conditions, guaranteeing that only axial forces were transmitted to the members. To save an appreciable amount of computation time, the joints were assumed to be symmetrical, and it was therefore only necessary to model half.

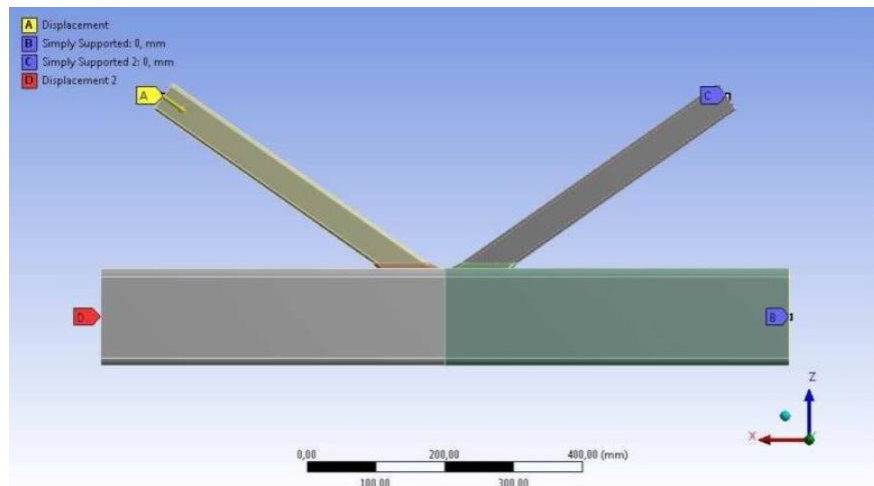


Figure 4. Global boundary conditions in FE Models.

### 3. Validation of Finite Element Modeling

Experimental test results from a pair of CIDECT projects developed at the University of Delft [40,41] were used to validate the model. These experiments included six tests carried out on RHS K-joint configurations with brace angles of  $45^\circ$ . The reports published force-indentation curves for one of the selected tests (named as Test 1) [40], but they were not published for the other five [41]. The braces did not include any holes for ventilation, and there was always a gap between the braces on the chord face. The gap between the braces was designed to avoid joint eccentricity and the corresponding moment caused by this. The only available data with respect to the weld throat of the specimens indicated that it was equal to the brace thickness, which is in accordance with the previously mentioned rule for modeling the welds. Figure 5 shows the joint configuration used in the tests with the global dimensions of the connected members.

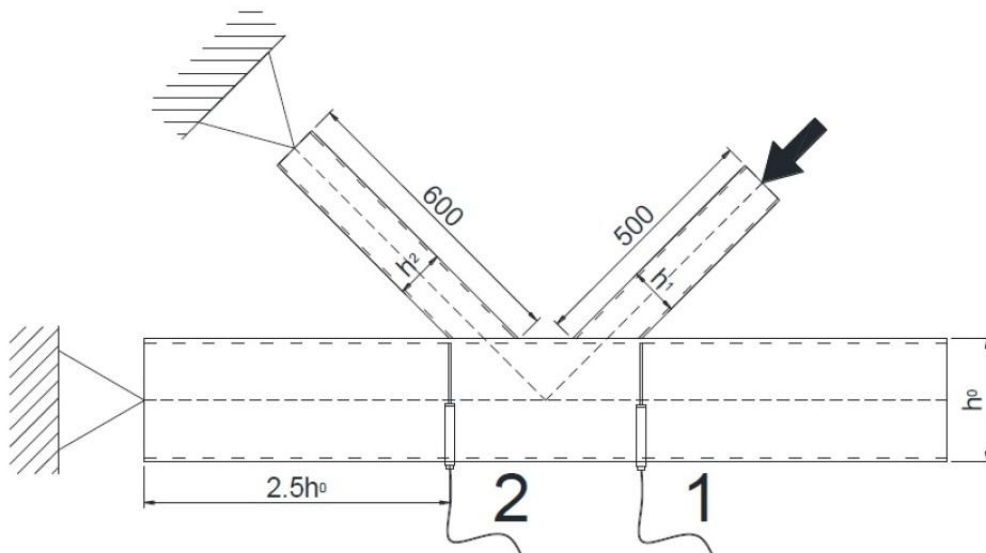


Figure 5. Tested K-joint configuration.

In the numerical model, the actual stresses and strains ( $\sigma_{act}$ ,  $\epsilon_{act}$ ) of the steel were taken, rather than the engineering values ( $\sigma_{eng}$ ,  $\epsilon_{eng}$ ) from the standard tests. The equations for transforming the values from engineering values to actual values are presented as Equations (3) and (4), below.

$$\epsilon_{act} = \ln(\epsilon_{eng} + 1) \quad (3)$$

$$\sigma_{act} = \sigma_{eng}(\varepsilon_{eng} + 1) \quad (4)$$

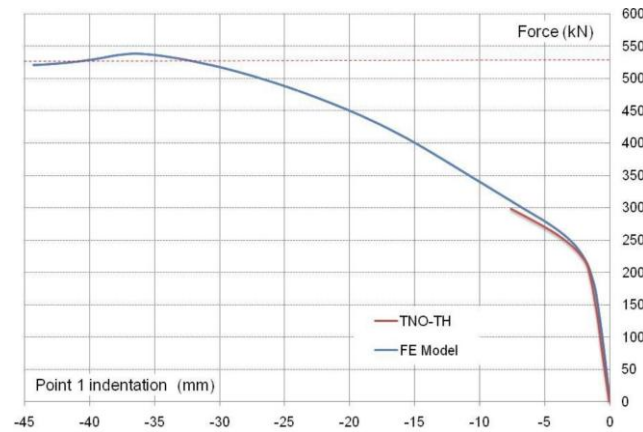
The nominal steel grade was S275, with hot-finished tubes for tests 1, 2, 5 and 6, but cold-formed tubes for tests 3 and 4. To simulate the material behavior, isotropic bilinear hardening was assumed [42]. In the case of tests 3 and 4, a proportionality limit of 85% of the elastic limit was adopted, in accordance with [43]. The material properties ( $f_y$  and  $f_u$ ) of the cold-formed RHS were obtained in Delft from stub column tests. Therefore, the average strain hardening, which primarily affects the corner area, is already considered, and it is not necessary to use additional procedures such as those presented in [44]. Table 1 presents the dimensions of the joint members, the relative gap regarding the chord width ( $g/b_0$ ), the yield limit  $f_y$  and the ultimate strength  $f_u$ , and the tangent modulus (the slope of the strengthening stage) for the six tests. For weld modeling, the same material properties as those of the corresponding welded brace member were adopted. Some previous research [24,38] carried out in similar situations has confirmed that differences when the base material properties of the steel are also used to model the welds are not noticeable. Although some gaps were smaller than those in EN-1993-1-8 [4], the tests were carried out prior to the formulation of the code, and they were used in this research only for validation of the numerical model.

**Table 1.** RHS members in tests and material properties [40,41].

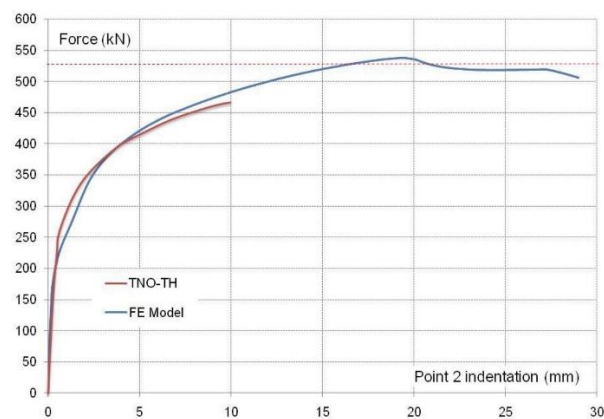
Test No	Gap ( $g/b_0$ )	Joint Members	$f_y$ [N/mm <sup>2</sup> ]	$f_u$ [N/mm <sup>2</sup> ]	Tangent Modulus [N/mm <sup>2</sup> ]
1	0.10	Chord: 258 × 258 × 8.4	289	409	1110
		Comp. Brace: 99.4 × 99 × 6.0	337	402	802
		Tension Brace: 103 × 99 × 5.2	317	405	932
2	0.43	Chord: 100 × 100 × 3.8	261	363	963
		Braces: 40 × 40 × 4.0	279	383	996
3	0.15	Chord: 100 × 100 × 4.1	462	512	1291
		Braces: 60 × 60 × 4.2	443	587	1813
4	0.15	Chord: 99.8 × 99.8 × 4.3	333	373	907
		Braces: 59.7 × 59.7 × 4.4	376	411	958
5	0.10	Chord: 102 × 102 × 3.9	363	520	1440
		Braces: 64 × 64 × 3.3	369	511	1350
6	0.10	Chord: 102 × 102 × 4.2	321	501	1550
		Braces: 64 × 64 × 4.0	349	401	729

When validating the model, it is important to take into account the joint stiffness and not only the joint resistance. Therefore, complete force-displacement curves were recorded from the simulation of Test 1 and were compared with those available from the experiment [40]. Figures 6 and 7 plot these curves, showing very good agreement in terms of initial stiffness and maximum load between the test and the FE models. Both Figures 6 and 7 present the force applied on the compression brace member vs. the displacement as an indentation measured at points 1 and 2 in accordance with Figure 5. Figures 6 and 7 show the complete force-indentation curves obtained with the FE model (blue curves), but the curves available from the report for the tests carried out in Delft (red curves) are only plotted for indentations of between 8 and 10 mm. As the maximum load achieved during the tests is known from the report, these values were also plotted as a horizontal line in order to compare them with the maximum load predicted by the model, and a good agreement can be observed. Figures 6 and 7 also show a good agreement between the model and the test for the initial joint stiffness (both curves match very well in this zone). These figures present displacements at two points of the tested joint. No data were available from the tests with respect to deformations at other points for the purpose of comparison with those from the simulation. With respect to the failure mode, as mentioned above, the general configuration of the joints and the combination of braces and chords for the parametric study were selected to predominantly present “brace failure”. To faithfully reproduce the test, the model created

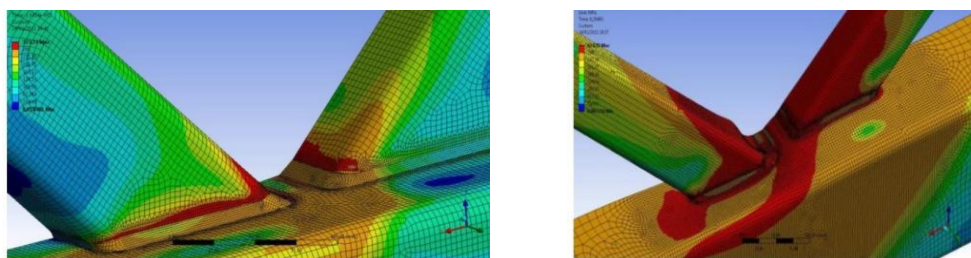
for this joint did not include any holes. Figure 8 shows the Von Mises stresses for the simulated K-joint when yielding was reached in some areas (on the left) and after large deformations (on the right). It can be seen that yielding started in the brace under compression above the weld and later spread to the chord.



**Figure 6.** Curve compression force vs. indentation at point 1.



**Figure 7.** Curve compression force vs. indentation at point 2.

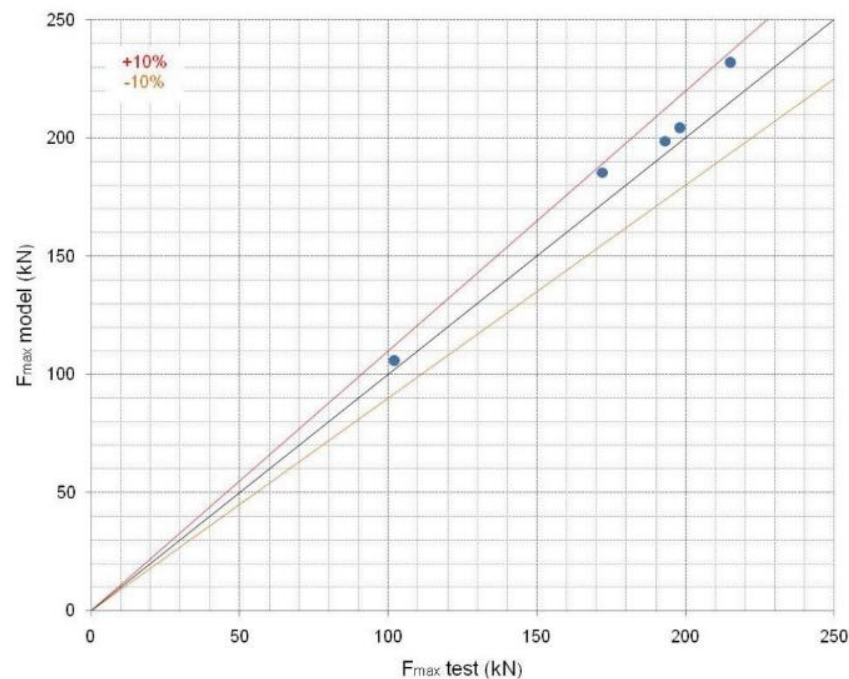


**Figure 8.** Von Mises stresses in the simulation of the K-joint.

A second validation to confirm the suitability of the numerical model was carried out by comparing the maximum loads obtained by the model with the results obtained in the experiments for Tests 2 to 6 (Table 1). The model was adapted to the corresponding dimensions and material properties of the specific joints. Table 2 presents the maximum loads obtained from the tests and simulations for the purpose of comparison. The percentage of deviation, which had a mean value of 5.1%, is also included in the table. Figure 9 shows the comparison of these results. The two lines above and below the diagonal indicating complete concordance represent deviations of up to 10%. The small differences registered confirm the validation of the model.

**Table 2.** Maximum load from tests and simulation.

Joint	2	3	4	5	6
Test [kN]	102	215	172	198	193
Model [kN]	105.9	232.1	185.3	204.3	198.6
Deviation %	3.8	7.9	7.7	3.2	2.9

**Figure 9.** Model vs. tests for 2nd validation.

The proposed numerical simulation did not include any initial cracks, and therefore, the occasional tensile failure in the braces or welds cannot be precisely simulated in terms of whether there are any defects or discontinuities that might lead to fracture. This limitation is typically assumed when these types of joints are modeled [39]. However, the other failure mechanisms (yielding and local buckling at the joint location), which can be grouped together under ‘brace failures’ or ‘brace effective width failures’, were well reproduced.

#### 4. Parametric Study of K- and N-joints Results and Discussion

After validation, the model was extended by means of a parametric study to take into account other K-joints and some N-joint configurations. All the new joints, initially without the vent holes, were combined with the three above described vent hole geometry. The complete program included eight K-joints plus three N-joints involving different sizes of rectangular hollow sections as chord members and square hollow sections as brace members. The K-joints were symmetrical, with brace angles of 45°, 55° and 60°. The diagonal brace in the N-joints had an angle of 45°. The purpose of this was to be able to analyze the influence of several variables linked to the geometry on the joint strength, together with the presence of the hole in the braces and its shape and position. Table 3 presents the member dimensions, gap, angles and some other relative geometrical variables considered in the extended models. The joint reference indicates the type and number of joints, along with the expected failure mode, as described below. For every joint, a set of four options, including the three types of vent hole as well as the same joint without any holes, were studied. That means that 44 joints were analyzed. All these joints avoided eccentricities due to the coincidence of the chord and brace axes.

**Table 3.** Joint dimensions in the extended model.

Joint	Chord RHS ( $b_0 \times h_0 \times t_0$ )	Braces SHS ( $b_1 \times t_1$ )	$\beta$ ( $b_1/b_0$ )	$\gamma$ ( $b_0/2t_0$ )	Gap [mm]	( $g/b_0$ )	Angle [°]
KB1	60 × 80 × 5	30 × 3	0.5	6	37.6	0.62	45
KB2	60 × 80 × 5	40 × 3	0.66	6	23.4	0.39	45
KC3	60 × 80 × 4	40 × 3	0.66	7.5	23.4	0.39	45
KB4	60 × 80 × 5	30 × 3	0.5	6	19.4	0.32	55
KB5	80 × 100 × 5	40 × 3	0.5	8	43.4	0.54	45
KC6	80 × 100 × 5	40 × 4	0.5	8	43.4	0.54	45
KC7	80 × 100 × 5	40 × 5	0.5	8	43.4	0.54	45
KC8	60 × 110 × 5	30 × 3	0.5	6	28.8	0.48	60
NC9	60 × 110 × 4	30 × 3	0.5	7.5	18.8	0.31	45–90
NP10	60 × 110 × 5	30 × 3	0.5	6	18.8	0.31	45–90
NP11	60 × 110 × 6	30 × 3	0.5	5	18.8	0.31	45–90

Table 4 shows the main dimensions of the three vent holes considered in the extended model according to Figure 2. In this part of the research, a nominal S275 was chosen, assuming bilinear behavior of the steel with a tangent modulus (the slope of the hardening stage) of 1330 N/mm<sup>2</sup>.

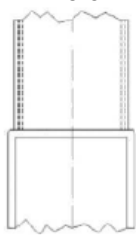
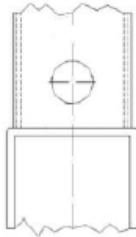
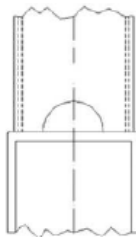
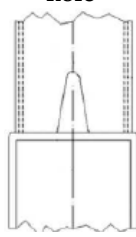
**Table 4.** Vent hole dimensions in the extended model.

Joint	Chord ( $b_0 \times h_0 \times t_0$ )	Braces ( $b_1 \times t_1$ )	Circular $D$ [mm]	Semi-Circular $D$ [mm]	V-Notch $B$ [mm]	$H$ [mm]
KB1	60 × 80 × 5	30 × 3	8.5	12.0	3.3	12.8
KB2	60 × 80 × 5	40 × 3	12.0	17.0	4.5	20.0
KC3	60 × 80 × 4	40 × 3	8.5	12.0	3.3	12.8
KB4	60 × 80 × 5	30 × 3	8.5	12.0	3.3	12.8
KB5	80 × 100 × 5	40 × 3	12.0	17.0	4.5	20.0
KC6	80 × 100 × 5	40 × 4	11.3	16.0	4.3	18.5
KC7	80 × 100 × 5	40 × 5	10.6	15.0	4.0	17.1
KC8	60 × 110 × 5	30 × 3	8.5	12.0	3.3	12.8
NC9	60 × 110 × 4	30 × 3	8.5	12.0	3.3	12.8
NP10	60 × 110 × 5	30 × 3	8.5	12.0	3.3	12.8
NP11	60 × 110 × 6	30 × 3	8.5	12.0	3.3	12.8

In these kinds of joints, it is common to establish as a limit the load at which the indentation in the chord face reaches 3% of the chord width ( $b_0$ ) [45]. Therefore, both the maximum load supported by the joint and the load corresponding to the indentation criterion of 3% were registered. These data are presented in Table 5 for the 44 configurations corresponding to the combinations of the type of joint and the shape of the vent hole. The criterion of 3% indentation always presented a lower result than the maximum load in the joint. Table 5 also includes the predicted failure mode according to formulation in EN-1993-1-8 [4]. These failure modes are: BF (brace failure), CF (chord plastification), and PS (punching shear). However, this was not conclusive for joints 1 to 5, because the values for the ultimate loads based on 3% indentation and those based on the maximum load supported by the joint were very close to one another, with differences of less than 5%.

Table 6 presents the deviations of maximum loads achieved using both criteria when joints with different vent holes are compared to joints without any holes. The results from Tables 5 and 6 indicate that joint resistance hardly changes with different shapes or positions of the vent holes, or when compared with the same joint without any holes. If the 3% $b_0$  criterion is applied, deviations of mean values for different geometries when compared with joints without vent holes are lower than 1% in the case of circular holes, 2.2% for semi-circular holes, and only 3.4% when using V-notched holes.

**Table 5.** Load for an indentation of  $3\%b_0$  and maximum load in the joints [kN].

Joint	Without hole		Circular hole		Semi-circular hole		Vnotched hole		Type of Failure
									
KB1	85.6	88.8	84.7	87.8	84.3	88.1	82.5	86.8	BF
KB2	125.1	125.7	124.8	126.2	123.9	124.9	121.9	123.5	BF
KC3	100.9	108.9	100.8	107.6	96.7	107.3	96.9	106.0	CF
KB4	75.5	90.6	75.3	89.8	74.4	89.5	72.8	88.7	BF
KB5	94.5	107.0	92.3	105.9	92.6	106.5	91.5	105.2	BF
KC6	105.2	142.0	103.4	141.7	102.5	140.6	101.3	138.6	CF
KC7	112.7	183.5	111.7	184.1	109.3	181.7	109.2	178.8	CF
KC8	74.1	95.5	74.4	94.4	72.6	94.4	71.5	93.8	CF
NC9	42.8	99.9	42.7	99.5	41.4	96.7	42.0	98.2	CF
NP10	67.0	99.8	65.7	100.1	64.2	98.0	64.1	98.8	PS
NP11	91.2	102.6	91.1	102.7	87.2	101.3	87.7	101.7	PS

[BF] Brace failure, [CF] Chord failure, [PS] Punching shear.

**Table 6.** Deviations of loads for different vent holes with respect to joints without holes.

	Type of vent hole					
	Circular		Semi-circular		V-notched	
	$3\%b_0$	Max. load	$3\%b_0$	Max. load	$3\%b_0$	Max. load
Mean of deviation [%]	−0.78	−0.45	−2.25	−1.30	−3.43	−1.91
Maximum deviation [%]	−2.34	−1.2	−4.23	−3.23	−4.31	−2.69

In Eurocode 3 [4], there is an analytical formulation for calculating the joint resistance for joints without any vent holes. If the results from Table 5 are compared with the code predictions, the following facts become evident. For most of the joints, the results obtained using the code formulation exceed those obtained by simulation with the  $3\%b_0$  criterion with a mean deviation of 8.8%, but are lower than results obtained for the maximum load in the joint using the numerical model. When the predicted failure mode in the code is brace failure, the results of maximum load criterion are closer to the analytical formulation. In contrast, for the analyzed N-joints, when a different failure mode is predicted, the  $3\%b_0$  criteria showed a better agreement with the equations.

Figure 10 shows in one graphic the three comparisons of maximum load in joints without any holes vs. those joints with circular, semi-circular or V-notched vent holes. In the same way, Figure 11 plots in one graphic these three comparisons of loads achieved by the joints, but in consideration of the  $3\%b_0$  indentation criterion. For the sake of greater clarity, Figure 12 presents this last comparison of loads in a bar diagram, allowing the identification of every joint considered in the study. From these three last figures, it is possible to point out that neither the hole presence nor the shape and position of the considered holes imply a significant strength reduction in the joints.

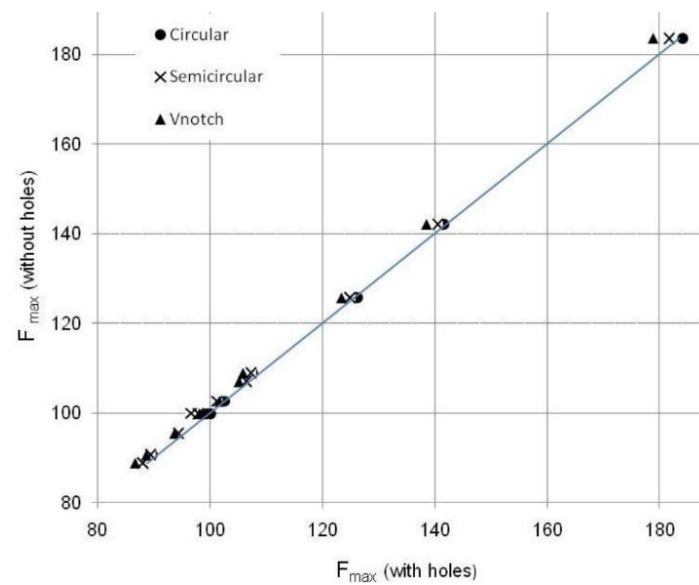


Figure 10. Comparison of maximum load in the joints with and without vent holes.

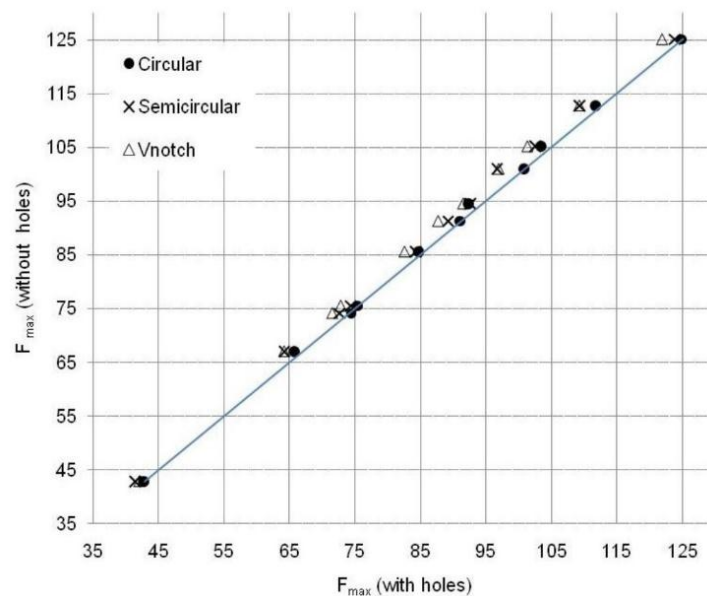


Figure 11. Comparison of load for a 3%  $b_0$  indentation in joints with and without vent holes.

In addition to the presence, shape and position of the vent holes in the joint, some other variables were also analyzed to ascertain their effect on joint resistance. Therefore, it was observed that thicker brace thickness,  $t_1$ , produced a predictable increase in the joint resistance, but also a different failure mode, changing from local buckling in the brace member to chord yielding. A bigger ratio between the widths of the brace and the chord—that is, the  $\beta$  ratio—implied higher joint resistance, as proposed by the Eurocode formulation. With respect to the influence of brace angle, it was observed that joint resistance decreases when brace angle increases, confirming prior studies [46]. Also, the predicted failure mode changed from brace failure to chord plastification in the case of brace angles of  $60^\circ$ . In the case of the N-joints, the main parameter considered apart from the vent hole shape was chord thickness. The observed maximum loads achieved by the joints showed a clear increase with chord thickness.

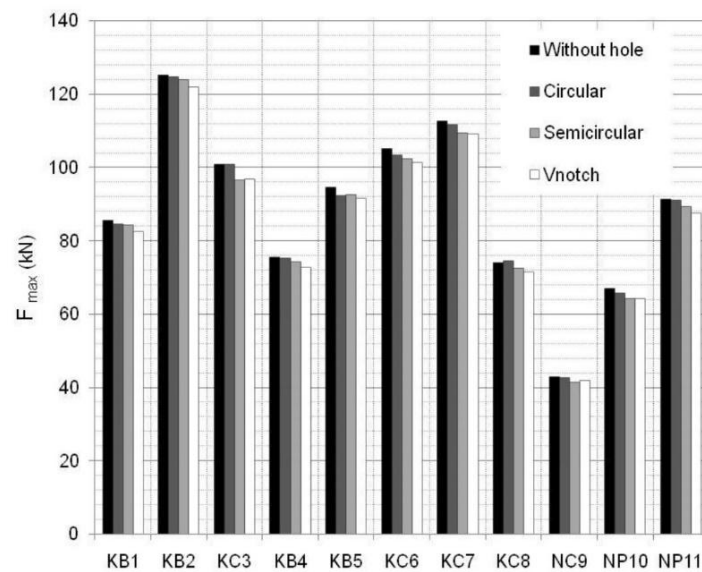


Figure 12. Comparison of maximum load for a 3%  $b_0$  indentation.

Figures 13–16 show some examples of failure modes for four different joint configurations, combining type of joint, shape of vent hole, and brace angles. Some of the failure modes are easy to identify, such as the chord failure shown in Figure 15, which fits well with the failure mode predicted by the code formulation. For others, there was a kind of combined failure mode, which included yielding and local buckling at the joint location and which may be grouped together under brace effective width failure.

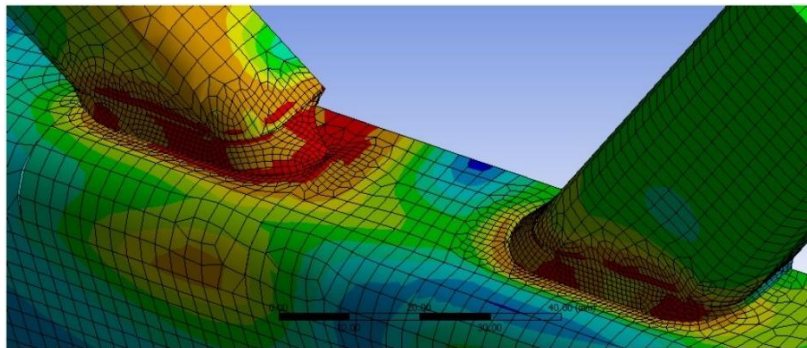


Figure 13. Failure in joint KB1 with a semi-circular hole and brace angles of 45°.

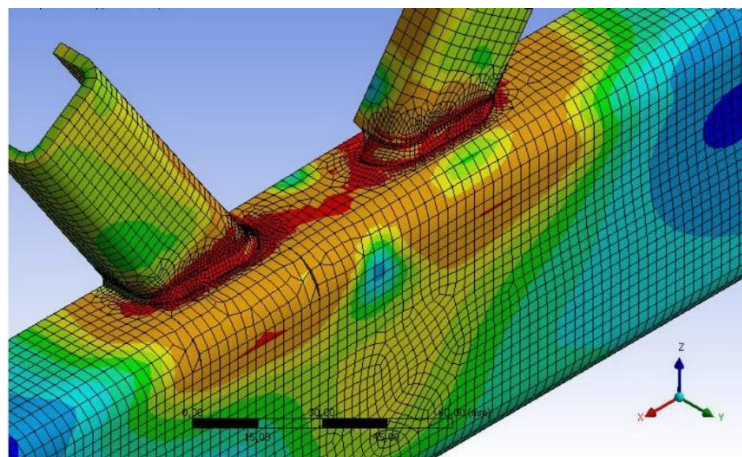
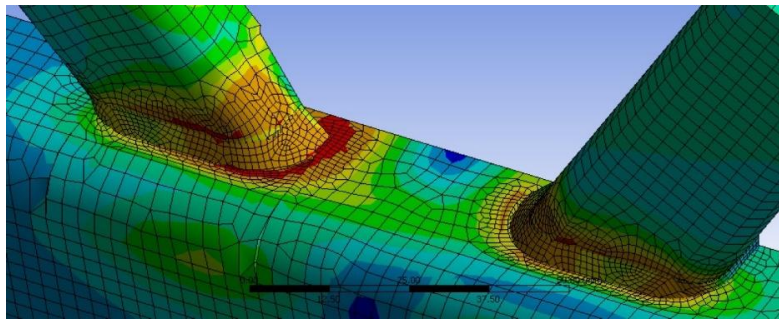
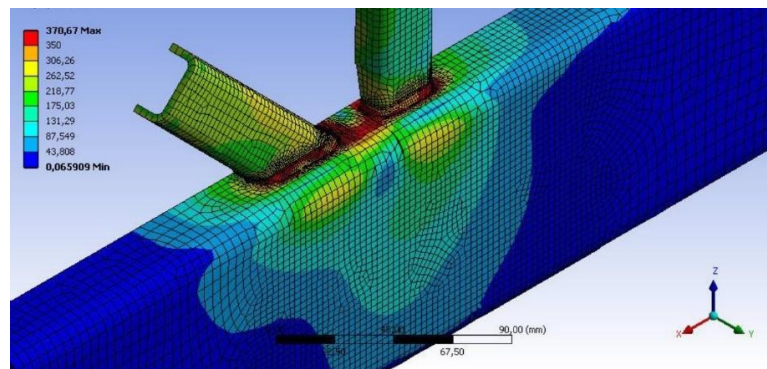


Figure 14. Failure in joint KB4 with semi-circular hole and brace angles of 55°.



**Figure 15.** Failure in joint KC8 with V-notched hole and brace angles of  $60^\circ$ .



**Figure 16.** Failure in joint NP10 with V-notched hole and braces angles of  $45\text{--}90^\circ$ .

## 5. Conclusions

In this research, a FE model was successfully validated on the basis of experimental results and then extended to be able to analyze the behavior of RHS K- and N-joints in lattice girders when the brace members include the ventilation holes necessary for the hot-dip galvanizing process. Different vent hole shapes, which allow the recovery of fluid after the zinc bath, were evaluated in order to achieve good efficiency during galvanization. Complete recovery is only possible when the welds connecting the brace and the chord are cut by the orifices. This work is focused on joints prone to failure due to local buckling in the brace member at the joint location (effective width failure at the compression brace) and chord plastification. The following conclusions may be drawn from this study:

- The developed FE simulation accurately reproduced the actual behavior of the analyzed joints, showing good agreement with the experimental results when the welds were modeled. Therefore, this model, based on shell elements, is adequate for simulating the RHS K- and N-joints in lattice girders and for predicting the strength and stiffness when fracture in welds can be avoided.
- There is a reasonable agreement with the Eurocode equations, confirming that FEA is a useful tool for obtaining appropriate results regarding joint behavior.
- In the numerical simulation, different combined failure modes were observed, but these were never dependent on the presence of a vent hole or on the shape of the vent hole.
- The local buckling present in a brace failure occurs away from the vent holes and the welds; therefore, in these cases, the presence of holes has no influence on joint resistance.
- If the thickness ratio between the brace and the chord results in chord plastification, the effect of the presence of a hole is also negligible with respect to joint resistance.
- The presence of a ventilation hole for the hot-dip galvanizing process such as those considered in this study does not significantly affect the joint resistance.
- Based on the small differences observed for joint resistance, it is possible to affirm that it does not matter what type of vent holes are used for the galvanization process. All the analyzed hole shapes presented fair performance in terms of the mechanical strength of the joint. Although the

shapes that cut the brace-chord weld exerted slightly more influence over the resistance than holes at some distance, all of them could be proposed to be valid solutions for machining vent holes.

- Taking into account the above-mentioned conclusions, we can offer some recommendations for engineers when designing galvanized lattice girders with RHS. They may choose any of the considered vent hole configurations, observing only the suggested filling areas. Therefore, certain preferences throughout the manufacturing process could be reasons for making a final decision.

This research work, carried out as part of a Cidect project, was discussed, reviewed and approved by the group of experts in the Cidect Technical Commission.

**Author Contributions:** Conceptualization, M.A.S. and C.L.-C.; Methodology, C.L.-C. and J.S.; Validation, F.L.G. Formal Analysis, C.L.-C. and F.L.G.; Writing—Original Draft Preparation, M.A.S. and T.W.; Writing—Review & Editing, M.A.S., T.W. and J.S.; Funding Acquisition, M.A.S.

**Funding:** This research was funded by Spanish MINISTERIO DE CIENCIA E INNOVACION, grant number BIA2017-83467-P, by the Cidect under project 5BX and by the European General Galvanizers Association.

**Acknowledgments:** The authors would like to acknowledge the IEMES Research Group from the University of Oviedo and the CASE from the University of Sydney for their backing. Besides, they would also like to thank Swanson Analysis Inc. for their assistance with the use of ANSYS University program.

**Conflicts of Interest:** “The authors declare no conflict of interest”. “The funders had no role in the design of the study; in the collection, analyses, or interpretation of data; in the writing of the manuscript, or in the decision to publish the results”.

## Nomenclature

HDG	hot-dip galvanizing
HSS	hollow structural section
RHS	rectangular hollow section
SHS	square hollow section
$b$	width of the hollow section
$h$	depth of the hollow section
$t$	thickness of the hollow section
$g$	gap of the joint
$\beta$	ratio of widths ( $b_i/b_0$ )
$\gamma$	ratio ( $b_0/(2t_0)$ )
$f_u$	ultimate strength
$f_y$	yield strength
$D$	circular vent hole diameter
$H$	height of V-notched vent hole
$B$	half opening of V-notched vent hole
$R$	radius of V-notched vent hole
$\alpha$	half angle of V-notched vent hole
$t_w$	weld throat
$\varepsilon_{act}$	actual strain
$\varepsilon_{eng}$	engineering strain
$\sigma_{eng}$	engineering stress
$\sigma_{act}$	actual stress

## Subscripts

$i$	denoting the brace
$o$	denoting the chord
act.	actual value
eng.	engineering value

## References

1. Glinde, H. *Galvanizing Explained. The Misunderstood Process*; Hot Dip Galvanizing Magazine; Galvanizers Association: Birmingham, UK, 2013.

2. American Galvanizers Association. Galvanize It! Online seminar: ‘Sustainable development & hot-dip galvanizing’. Available online: <http://www.galvanizeit.org/sustainable-development-and-hot-dip-galvanizing> (accessed on 1 February 2018).
3. Cornish, R. General Galvanizing in North America-Association, key metrics and markets. In Proceedings of the Proceedings of 9th Asia Pacific General Galvanizing Conference, Singapore, 1–2 November 2018.
4. CEN, EN-1993-1-8:2005, *Eurocode 3: Design of Steel Structures. Part 1–8*; European Committee for Standardization: Brussels, Belgium, 2005; ISBN 978-3-433-03216-9.
5. AISC. *Specification for Structural Steel Buildings*; ANSI/AISC 360-10; American Institute of Steel Construction: Chicago, IL, USA, 2010.
6. AWS D1.1/D1.1 M: *Structural Welding Code-Steel*, 22th ed.; American Welding Society: Miami, FL, USA, 2010.
7. CEN, EN-10219-2:2006 *Cold Formed Welded Structural Hollow Sections of Non-Alloy and Fine Grain Steels. Part 1: Technical Delivery Conditions; Part 2: Tolerances, Dimensions and Sectional Properties*; European Committee for Standardization: Brussels, Belgium, 2006.
8. CEN, EN-10210-2:2006 *Hot Finished Structural Hollow Sections of Non-Alloy and Fine Grain Steels. Part 1: Technical Delivery Conditions; Part 2: Tolerances, Dimensions and Sectional Properties*; European Committee for Standardization: Brussels, Belgium, 2006.
9. Packer, J.A.; Wardenier, J.; Zhao, X.L.; Van der Vegte, G.J.; Kurobane, Y. *Design Guide 3 for Rectangular Hollow Section (RHS) Joints under Predominantly Static Loading*, 2nd ed.; LSS Verlag: Köln, Germany, 2009.
10. Packer, J.A.; Henderson, J.E. *Hollow Structural Section Connections and Trusses, A Design Guide*; Canadian Institute of Steel Construction: Markham, ON, Canada, 1997.
11. Dutta, D.; Wardenier, J.; Yeomans, N.; Sakae, K.; Bucak, Ö.; Packer, J.A. *Design Guide 7: For Fabrication, Assembly and Erection of Hollow Section Structures*; TÜV-Verlag: Cologne, Germany, 1998.
12. IIW, 2009. *Static Design Procedure for Welded Hollow Section Joints—Recommendations*, 3rd ed.; Commission XV, IIW Doc. XV-1329-09, IIW Annual Assembly; International Institute of Welding: Singapore, 2009.
13. Wardenier, J.; Packer, J.A.; Zhao, X.L.; Van der Vegte, G.J. *Hollow Sections in Structural Applications*, 2nd ed.; Bouwen Met Staal: Rotterdam, The Netherlands, 2010.
14. Wardenier, J. *Hollow Section Joints*; Delft University Press: Delft, The Netherlands, 1982.
15. Puthli, R.; Packer, J.A. Structural design using cold-formed hollow sections. *Steel Constr.* **2013**, *6*, 150–157. [[CrossRef](#)]
16. Ritakallio, P.O. Cold-formed high-strength tubes for structural applications. *Steel Constr.* **2012**, *5*, 158–167. [[CrossRef](#)]
17. Cook, M. European General Galvanizers Association. Galvanizing in the European Union. In Proceedings of the Congresso Brasileiro de Galvanização ‘GalvaBrasil Conference’, Sao Paulo, Brazil, 22–23 October 2013.
18. Zedet, A. European General Galvanizers Association. Challenges and Prospects for General Galvanizing in Europe. In Proceedings of the 9th Asia Pacific General Galvanizing Conference, Singapore, 8–11 September 2013.
19. Langill, T.J. Mechanical Properties of Hot-Dip Galvanized Steel. In Proceedings of the American Society of Civil Engineers Congress, Structures, Austin, TX, USA, 24–27 June 2009.
20. Coni, N.; Gipiela, M.L.; D’Oliveira, A.S.C.M.; Marcondes, P.V.P. Study of the Mechanical Properties of the Hot Dip Galvanized Steel and Galvalume. *J. Braz. Soc. Mech. Sci. Eng.* **2009**, *31*, 319–326. [[CrossRef](#)]
21. Feldmann, M.; Pinger, T.; Schäfer, D.; Pope, R.; Smith, W.; Sedlacek, G. *Hot-Dip-Zinc-Coating of Prefabricated Structural Steel Components*; JRC Scientific and Technical Reports; European Commission: Brussels, Belgium, 2010.
22. Sun, M.; Packer, J.A. Hot-dip galvanizing of cold-formed steel hollow sections: A state-of-the-art review. *Front. Struct. Civ. Eng.* **2019**, *13*, 49–65. [[CrossRef](#)]
23. Berto, F.; Mutignani, F.; Pitarello, L. Effect of hot-dip galvanization on the fatigue behaviour of structural steel. In Proceedings of the 21st European Conference on Fracture, Procedia Structural Integrity, Catania, Italy, 20–24 June 2016.
24. Lozano, M.; Serrano, M.A.; López-Colina, C.; Gayarre, F.L.; Suárez, J. The Influence of the Heat-Affected Zone Mechanical Properties on the Behaviour of the Welding in Transverse Plate-to-Tube Joints. *Materials* **2018**, *11*, 266. [[CrossRef](#)] [[PubMed](#)]

25. Landa, P.; Iglesias, G. Cidect Project 14B. Monograph on Hot-Dip Galvanized Tubular Structures: Design Recommendations for Holes Due to Galvanizing Process. Available online: [http://www.cidect.org/en/Research\\_Projects/](http://www.cidect.org/en/Research_Projects/) (accessed on 17 August 2018).
26. Serrano, M.A.; López-Colina, C.; Iglesias, G. Cidect project 5BX. Static Strength of RHS K-Joints in Which Brace Members May be Affected by Vent Holes for Truss Hot-Dip Galvanizing, Final Report. Available online: [http://www.cidect.org/en/Research\\_Projects/](http://www.cidect.org/en/Research_Projects/) (accessed on 17 August 2018).
27. Serrano-López, M.A.; López-Colina, C.; del Coz-Díaz, J.J.; Gayarre, F.L. Static behavior of compressed braces in RHS K-joints of hot-dip galvanized trusses. *J. Constr. Steel Res.* **2013**, *89*, 307–316. [[CrossRef](#)]
28. del Coz, D.; Serrano-López, M.A.; López-Colina Pérez, C.; Álvarez Rabanal, F.P. Effect of the vent hole geometry and welding on the static strength of galvanized RHS K-joints by FEM and DOE. *Eng. Struct.* **2012**, *41*, 218–233. [[CrossRef](#)]
29. Lee, M.M.K. Strength, stress and fracture analyses of offshore tubular joints using finite elements. *J. Constr. Steel Res.* **1999**, *51*, 265–286. [[CrossRef](#)]
30. Lee, M.M.K.; Dexter, E.; Kirkwood, M. Strength of moment-loaded tubular T/Y-joints in offshore platforms. *Struct. Eng.* **1995**, *73*, 239–246.
31. Lalani, M. Post-yield and post-peak behaviour of tubular joints in offshore structures. In Proceedings of the 5th international Symposium on Tubular Structures, Nottingham, UK, 25–27 August 1993; pp. 446–454.
32. Van der Vegte, G.J.; De Konig, C.M.H.; Puthli, R.S.; Wardenier, J. Numerical simulations of experiments on multiplanar tubular steel X-joints. *Int. J. Offshore Polar Eng.* **1991**, *1*(3). Document ID: ISOPE-91-01-3-200.
33. Lee, M.M.K.; Wilmschurst, S.R. Numerical modelling of CHS joints with multiplanar double-K configuration. *J. Constr. Steel Res.* **1995**, *32*, 281–301. [[CrossRef](#)]
34. Suo, Y.; Yang, W.; Chen, P. Study on Hysteresis Model of Welding Material in Unstiffened Welded Joints of Steel Tubular Truss Structure. *Appl. Sci.* **2018**, *8*, 1701. [[CrossRef](#)]
35. López-Colina, C.; Serrano-López, M.A.; López-Gayarre, F.; Suárez, F.J. Resistance of the component ‘lateral faces of RHS’ at high temperature. *Eng. Struct.* **2010**, *32*, 1133–1139. [[CrossRef](#)]
36. López-Colina, C.; Serrano-López, M.A.; López-Gayarre, F.; del Coz Díaz, J.J. Stiffness of the component ‘lateral faces of RHS’ at high temperature. *J. Constr. Steel Res.* **2011**, *67*, 1835–1842. [[CrossRef](#)]
37. López-Colina, C.; Serrano, M.A.; Gayarre, F.L.; González, J. The component ‘lateral faces of RHS’ under compression at ambient and high temperature. *Int. J. Steel Struct.* **2014**, *14*, 13–22. [[CrossRef](#)]
38. Serrano-López, M.A.; López-Colina, C.; González, J.; López-Gayarre, F. A Simplified FE Simulation of Welded I Beam-to-RHS Column Joints. *Int. J. Steel Struct.* **2016**, *16*, 1095–1105. [[CrossRef](#)]
39. Van der Vegte, G.J.; Wardenier, J.; Puthli, R.S. FE analysis for welded hollow-section joints and bolted joints. *Struct. Build* **2010**, *163*, 427–437. [[CrossRef](#)]
40. Wardenier, J.; De Koning, C.H.M. *Rig Comparison Tests for Welded Joints*; Cidect Project 5S-76-33, TNO; The University of Delft: Delft, The Netherlands, 1976.
41. Wardenier, J.; Stark, J.W.B. *The Static Strength of Welded Lattice Girder Joints in Structural Hollow Sections, Revised Final Report*; Cidect Project 5Q/78/4, TNO; The University of Delft: Delft, The Netherlands, 1978.
42. Yang, W.; Lin, J.; Gao, N.; Yan, R. Experimental Study on the Static Behavior of Reinforced Warren Circular Hollow Section (CHS) Tubular Trusses. *Appl. Sci.* **2018**, *8*, 2237. [[CrossRef](#)]
43. Outinen, J.; Kaitila, O.; Mäkeläinen, P. *Finite Element Modeling of Cold-Formed Steel Members at High Temperature*; Helsinki University of Technology Laboratory of Steel Structures Publications: Helsinki, Finland, 2002.
44. López-Colina, C.; Serrano, M.A.; Lozano, M.; Gayarre, F.L.; Suárez, J. Simplified Models for the Material Characterization of Cold-Formed RHS. *Materials* **2017**, *10*, 1043. [[CrossRef](#)] [[PubMed](#)]
45. Lu, L.H.; De Winkel, G.D.; Yu, Y.; Wardenier, J. Deformation limit for the ultimate strength of hollow section joints. In Proceedings of the 6th ISTS, Tubular Structures VI, Melbourne, Australia, 14–16 December 1994.
46. Serrano-López, M.A.; López-Colina, C.; Lozano, A.; Iglesias, G.; González, J. Influence of the angle in the strength of RHS K-joints in galvanized lattice girders. In Proceedings of the 14th ISTS, Tubular Structures XIV, London, UK, 12–14 September 2012; pp. 113–120.

